

Abnormal Hyperphosphorylation of Tau in Canine Immune-mediated Meningoencephalitis

MINGYUN SON^{1*}, YEON CHAE^{1*}, SANGGU KIM², TAESIK YUN¹, YOONHOI KOO¹,
DOHEE LEE¹, HAKHYUN KIM¹, MHAN-PYO YANG¹, BYEONG-TECK KANG¹ and SOOCHONG KIM²

¹Laboratory of Veterinary Internal Medicine, College of Veterinary Medicine,
Chungbuk National University, Cheongju, Republic of Korea;

²Laboratory of Veterinary Pathology, College of Veterinary Medicine,
Chungbuk National University, Cheongju, Republic of Korea

Abstract. *Background/Aim:* Tau is a microtubule-associated protein involved in the assembly and stabilization of microtubules. In human medicine, hyperphosphorylation of tau is associated with microtubule instability and is considered to play a role in the progression of multiple sclerosis (MS). MS is an autoimmune neurological disease that shares many characteristics, including pathological mechanisms, with canine meningoencephalitis of unknown etiology (MUE). With this background, this study investigated the presence of hyperphosphorylated tau in dogs with MUE and experimental autoimmune encephalomyelitis (EAE). *Materials and Methods:* In total, eight brain samples were examined from two neurologically normal dogs, three dogs with MUE, and three canine EAE models. Anti-(phospho-S396) tau antibody was used for immunohisto-chemistry, which stained hyperphosphorylated tau. *Results:* In normal brain tissues, hyperphosphorylated tau was not found. In all the dogs with EAE and one of the dogs with MUE, immunoreactivity for S396 p-tau was observed in glial cell cytoplasm and the background in the periphery of the

inflammatory lesion. Conclusion: These results suggest for the first time that tau pathology may be involved in the progression of neuroinflammation in dogs, similar to that in human MS.

Tau is a fundamental component involved in the binding and stability of microtubules and directly interacts with the proteins involved in microtubule-dependent transport (1). Its physiological roles are to stabilize microtubules and maintain the morphological and structural polarization of neurons (2). The phosphorylation of threonine, serine, and tyrosine at various domains within protein sequences regulates microtubule binding and the activity of tau (3). An adequate amount of phosphorylation of tau is required for it to function under normal conditions (4). In pathological conditions, however, phosphorylation of tau occurs more at serine, threonine, and tyrosine residues than normally, which is referred to as hyperphosphorylation (4, 5).

Hyperphosphorylated tau destabilizes and disrupts microtubules and inhibits axonal transport (6, 7). Hyperphosphorylated tau also promotes oligomerization, and such tau oligomers may induce mitochondrial damage and neurodegeneration (8, 9). Additionally, hyperphosphorylated tau catalyzes the formation of potentially toxic aggregates called neurofibrillary tangles (6, 10, 11). Although the exact pathological role of neurofibrillary tangles is not well understood, they are used as a marker of neurodegeneration (6). This pathology of tau based on hyperphosphorylation has long been studied as the major pathological mechanism of neurodegenerative disorders (6).

An association between neuroinflammation and hyperphosphorylation of tau was also found in experiments using various mouse models (12). The involvement of proinflammatory cytokines in tau hyperphosphorylation has also been investigated (13). In particular, the potential of phosphorylated tau (p-tau) as a biomarker of multiple sclerosis (MS), the most common neuroinflammatory disease

*These Authors contributed equally to this work.

Correspondence to: Byeong-Teck Kang, Laboratory of Veterinary Internal Medicine, College of Veterinary Medicine, Chungbuk National University, Cheongju 28644, Republic of Korea. Tel: +82 432613744, email: kangbt@chungbuk.ac.kr and Soochong Kim, Laboratory of Veterinary Pathology, College of Veterinary Medicine, Chungbuk National University, Cheongju 28644, Republic of Korea. Tel: +82 432491846, email: skim0026@cbnu.ac.kr

Key Words: Meningoencephalitis of unknown etiology, tau protein, microtubules, multiple sclerosis, phosphorylated tau, S396 p-tau.



This article is an open access article distributed under the terms and conditions of the Creative Commons Attribution (CC BY-NC-ND) 4.0 international license (<https://creativecommons.org/licenses/by-nc-nd/4.0>).

in humans, has been demonstrated by the identification of hyperphosphorylated tau and axonal loss in a mouse model of experimental autoimmune encephalomyelitis (EAE) and MS (14-17).

The term meningoencephalitis of unknown etiology (MUE) was introduced to refer to dogs with non-infectious inflammatory disorders of the central nervous system (CNS) without a histopathological diagnosis (18). Generally, MUE includes necrotizing leukoencephalitis, granulomatous meningoencephalomyelitis, and necrotizing meningoencephalitis (NME) (19).

Several etiologies have been theorized for the pathogenesis of MUE, and immune-mediated causes are considered the most likely (20). Recent data have shown that inflammatory lesions of MUE contain numerous T-lymphocytes positive for cluster of differentiation 3 (CD3) antigen (20). Similarly, MS is also regarded as a T-lymphocyte-mediated autoimmune disease and specifically related to myelin antigens in the CNS, which results in demyelination and axonal damage (21). Additionally, genetic studies have confirmed that genes involved in NME are highly correlated with genes that are related to human MS (22). Because of these similarities, MUE in dogs is considered a naturally occurring canine model of MS (22).

Although hyperphosphorylated tau has been found to be involved in MS and mouse EAE models, there is no evidence of its presence in dogs with neuroinflammatory diseases. Based on the similarities between human MS and canine MUE, it was hypothesized that hyperphosphorylation of tau may contribute to the development of canine neuroinflammatory diseases. Therefore, this study aimed to evaluate the presence of hyperphosphorylation of tau in canine MUE and EAE using immunohistochemistry (IHC).

Materials and Methods

Animals. This study was conducted on the brains of a total of eight dogs, including two neurologically normal dogs, three dogs with MUE, and three dogs with EAE (Table I). In all cases, brains were obtained for research use through donation with the consent of the owner at the time of elective euthanasia or death. Client-owned dogs with MUE and healthy dogs that presented to the Veterinary Teaching Hospital at Chungbuk National University, between November 2017 and November 2020 were evaluated. Two control dogs with no known neurological disease were included. Dogs with MUE were included when two or more of the following criteria were fulfilled: i) Clear clinical signs, ii) mononuclear pleocytosis of cerebrospinal fluid (CSF) (defined as a pleocytosis comprising at least 50% mononuclear cells with no other leukocyte type exceeding 25%), iii) magnetic resonance imaging (MRI) of CNS consistent with focal or multifocal disease most compatible with a non-infectious and inflammatory etiology (19). All dogs with MUE were confirmed by post-mortem histopathological examination.

Three beagle dogs (1-3 years old, weighing 8.5-11 kg; two males/one female; DooYeol Biotech, Seoul, Republic of Korea) were used for induction of EAE. All dogs were considered healthy

based on their physical examination, complete blood count, and serum chemistry profile. The dogs were acclimated at least 1 month before induction. They were housed under an artificial light cycle with illumination from 9:00 to 21:00. The relative humidity was maintained at 40±10%, and the temperature was sustained at 20±2°C. The air was ventilated at 10 cycles/h. Each dog was kept in an individual cage. The beagles were fed 300 g (once) per day of standard laboratory diet (Cargill Agri Purina Korea Inc., Sunghnam, Republic of Korea) and allowed access to water *ad libitum*.

The study on EAE was approved by the Institutional Animal Care and Use Committee (CBNUA-1466-20-01) of the Laboratory Animal Research Center of Chungbuk National University.

Induction of EAE. The brain tissue of one dog with EAE in this study and one client-owned dog with glioma were used in the EAE immunization protocol. EAE was induced referring to the methods used in previous studies (23-25). Before the induction of EAE, the two brain samples of glioma and EAE were stored at -80° after necropsy. The glioma tissue was used to induce EAE in two beagles (EAE-1 and EAE-2), and the brain tissue of EAE-1 was then used to induce EAE of the third beagle (EAE-3). Briefly, 8 g of forebrain tissues were homogenized in an ice-bath for 5 min with 4 ml of phosphate-buffered saline (PBS). The resulting suspension was emulsified with the same amount of Freund's complete adjuvant (Sigma-Aldrich, St. Louis, MO, USA); each milliliter of Freund's complete adjuvant contained 1 mg of heat-killed and dried *Mycobacterium tuberculosis* (H37Ra, ATCC 25177), 0.85 ml paraffin oil, and 0.15 ml mannide monooleate. Each dog was subcutaneously injected with 0.20 ml/kg homogenate in the bilateral axillary and inguinal regions under sedation with alfaxalone (3 mg/kg, intravenous; Alfaxan, Careside Co., Ltd., Seongnam, Republic of Korea). All dogs received a booster injection seven days later.

Clinical assessments. Each beagle was evaluated by a daily examination for neurological abnormalities and their general condition after the first injection of brain tissue. The neurological examination included mental status, gait analysis, postural reactions, cranial nerve examination, and spinal reflexes. The successful induction of EAE was based on the following criteria: i) Clear neurological signs or ii) abnormal CSF findings (increased protein concentration and nucleated cell pleocytosis).

Physical and neurological examinations were performed on dogs with MUE. The neurological examination was conducted for the mental status, gait analysis, postural reactions, cranial nerves, and spinal reflexes. Signs, history, clinical signs, the onset of clinical signs of dogs with MUE were obtained from questionnaires provided by clients. All medical records, including CSF analysis, therapeutic drugs, and survival times were reviewed individually.

MRI and CSF analysis. MRI was performed every 14 days after the first injection and immediately after the first clinical symptoms of EAE were identified. MRI was carried out using a 1.5-Tesla device (Signa Creator; GE Healthcare, Milwaukee, WI, USA). All beagles were injected intravenously with propofol (Provide® inj.; Myungmoon Pharm. Co., Ltd., Seoul, Republic of Korea) at 4 mg/kg to induce anesthesia and general anesthesia was maintained with isoflurane (Terrell™; Minrad Inc., Bethlehem, PA, USA). T1-Weighted (pre- and post-contrast), T2-weighted, and fluid-attenuated inversion recovery (FLAIR) images were acquired in the transverse

Table I. Signs and clinical features of control dogs, dogs with experimental autoimmune encephalomyelitis (EAE), and dogs with meningoencephalomyelitis of unknown etiology (MUE).

Group	Number	Breed	Sex	Age, years	Neurological signs	Onset of signs	Therapy	Survival time, days	DD
Control	1	Maltese	Neutered male	14	None	–	–	–	MMVD
	2	Cane Corso	Intact male	6	None	–	–	–	HI
EAE	1*	Beagle	Intact male	3	Stuporous mental state, tetra-paresis, anorexia	Acute	–	39	NLE
	2*	Beagle	Intact female	1	Depression, head turn, ataxia	Acute	–	35	NLE
	3*	Beagle	Intact male	2	Depression, head turn, ataxia	Acute	–	14	NLE
MUE	1	Maltese	Intact female	7	Head tilt, head turn, seizure	Acute	PDS+MMF	165	NME
	2	Maltese	Neutered female	4	Seizure, ataxia	Acute	PDS+MMF	1164	NME
	3	Yorkshire Terrier	Intact male	8	Head turn, seizure	Acute	PDS+MMF	317	NLE

DD: Definitive diagnosis; EAE: experimental autoimmune encephalomyelitis; HI: heartworm infection; MMF: mycophenolate mofetil; MMVD: myxomatous mitral valve disease; MUE: meningoencephalomyelitis of unknown etiology; NLE: necrotizing leukoencephalitis; NME: necrotizing meningoencephalitis; PDS: prednisolone. *These dogs were euthanized due to severe neurological deficiencies.

Table II. Characteristics of magnetic resonance imaging (MRI) and cerebrospinal fluid (CSF) in dogs with experimental autoimmune encephalomyelitis (EAE) and dogs with meningoencephalomyelitis of unknown etiology (MUE).

Group	Number	Distribution	Margin	Site	T2w	FLAIR	T1w	T1w(C)	CSF findings
EAE	1	Diffuse	Indistinct	Telencephalon	Hyperintense	Hyperintense	Isointense	X	Neutrophilic pleocytosis, elevated protein level
	2	Diffuse	Indistinct	Telencephalon	Hyperintense	Hyperintense	Isointense	X	NE
	3	Diffuse	Indistinct	Telencephalon	Hyperintense	Hyperintense	Isointense	X	Neutrophilic pleocytosis, elevated protein level
MUE	1	Focal	Indistinct	Metencephalon	Hyperintense	Hyperintense	Isointense	O	No pleocytosis, normal protein level
	2	Diffuse	Indistinct	Telencephalon, diencephalon	Hyperintense	Hyperintense	Isointense	X	Monocytic pleocytosis, normal protein level
	3	Diffuse	Indistinct	Telencephalon	Hyperintense	Hyperintense	Hypointense	X	Lymphocytic pleocytosis, normal protein level

(C): Post-contrast; FLAIR: fluid-attenuated inversion recovery; NE: not evaluated; O: contrast enhancement was confirmed; T1w/T2w: T1/T2-weighted image; X: contrast enhancement was not confirmed.

and sagittal planes. CSF analysis was performed every 7 days after the first injection and immediately after the first clinical signs of EAE were observed. In dogs with EAE, CSF collection was performed while maintaining general anesthesia with isoflurane (Terrell™; Minrad Inc.) after induction with propofol (4 mg/kg Provive® inj., intravenous; Myungmoon Pharm. Co. Ltd.). CSF was obtained from the cerebellomedullary cistern of two dogs with EAE (EAE-1 and EAE-3) using a 22-gauge spinal needle (B Braun, Melsungen, Germany). CSF was collected in polypropylene tubes

and stored at –80°C until further use. The collected CSF was used for testing for total protein (mg/dl), total nucleated cell count (cells/μl), and cytology.

MRI scans and CSF collection in the dogs with MUE were performed in the same manner as in dogs with EAE using a 0.3-Tesla unit (Airis II; Hitachi, Japan) or 1.5-Tesla unit (Signa Creator; GE Healthcare). Following the MRI scan, CSF was collected from each dog with MUE. CSF examination of dogs with MUE was performed using the same protocol as dogs with EAE.

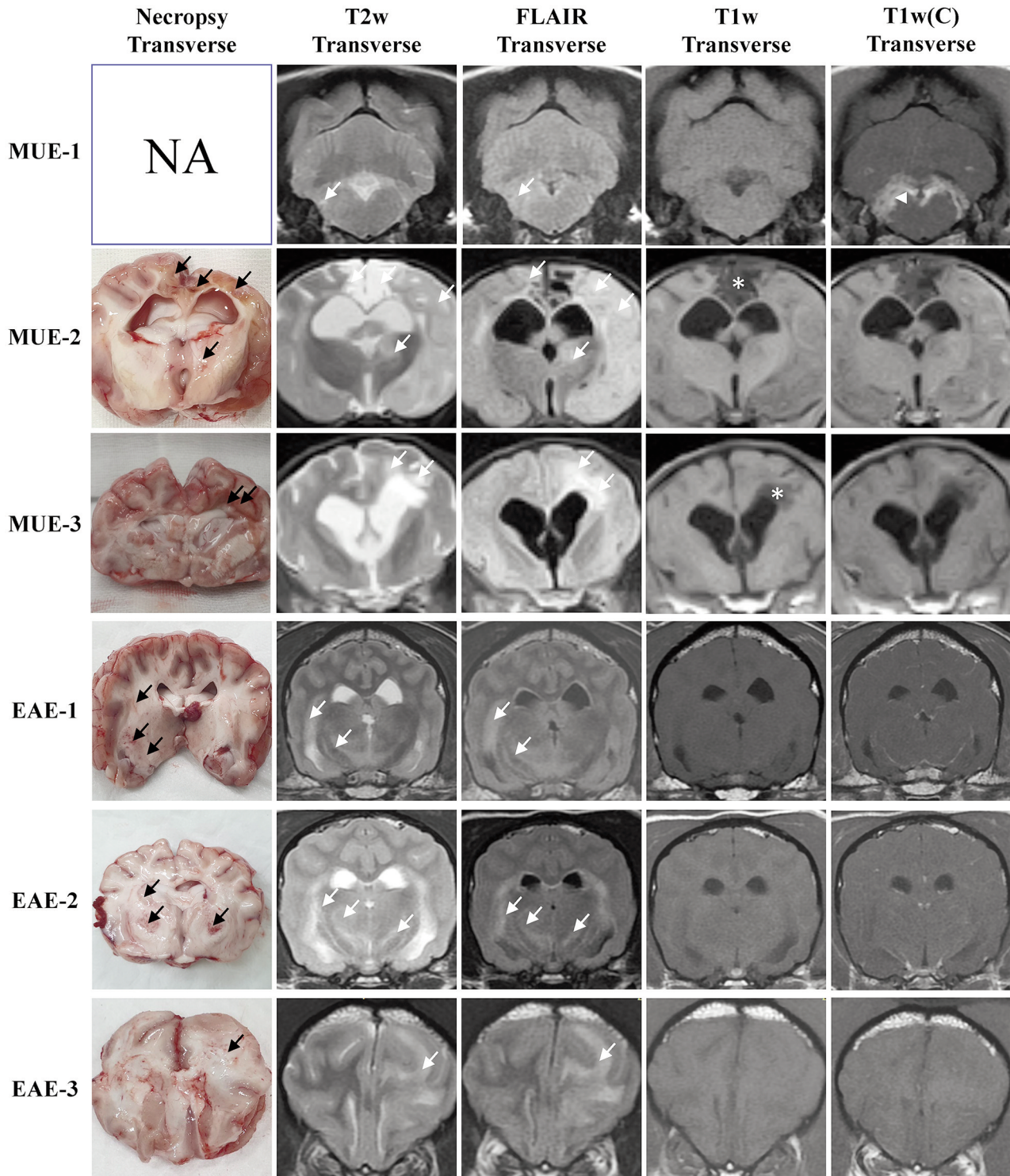


Figure 1. Brain magnetic resonance imaging (MRI) and necropsy findings in dogs with meningoencephalomyelitis of unknown etiology (MUE) and dogs with experimental autoimmune encephalomyelitis (EAE). The necropsy image of MUE-1 was not available (NA). Multifocal ill-defined diffuse lesions (white arrows) of the white matter were confirmed as hyperintense in T2-weighted (T2w) and fluid-attenuated inversion recovery images (FLAIR) in both the EAE and MUE groups. There were hypo- to isointense signals in T1-weighted (T1w) images of both groups, while peripheral contrast enhancement (arrowhead) was only observed in the medulla of MUE-1. Necrotic cavitory lesions (*) were identified in the cerebral cortex and cerebral white matter in MUE-2 and MUE-3. Gross examination revealed multiple ill-defined lesions with hemorrhagic atrophy (black arrows) in the gray and the white matter except for MUE-1. T1w(C): Post-contrast T1-weighted.

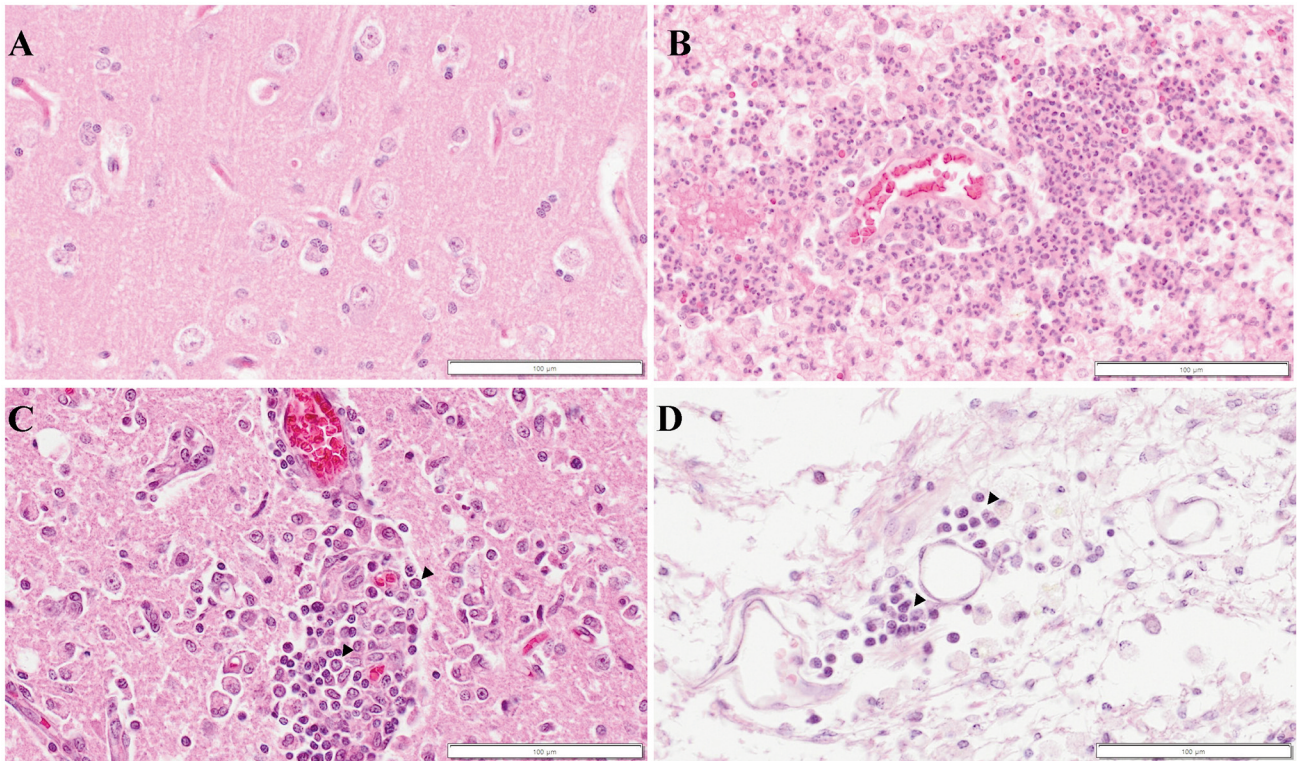


Figure 2. Hematoxylin and eosin staining of control dogs, dogs with meningoencephalomyelitis of unknown etiology (MUE), and dogs with experimental autoimmune encephalomyelitis (EAE). A: No histological abnormalities were observed in the frontal lobe of control-1. B: Parenchymal infiltration of neutrophils was observed in the frontal lobe of EAE-3. Malacic changes were rarely identified. C: Inflammatory perivascular cuffs were identified, and infiltration of lymphocytes was observed at the occipital lobe of MUE-1. D: Malacic changes and multifocal areas of inflammatory cell infiltration were observed in the frontal lobe of MUE-2. The scale bar represents 100 μ m.

Histopathology and IHC. All brains underwent dissection within 4 h post-mortem. Gross examinations were recorded, and the brain was then transversely sectioned into 4-mm-thick slices and compared to MRI findings. Samples containing the lesions were fixed in 10% formalin, embedded in paraffin, and serially sectioned into 4 μ m thick slices. Hematoxylin and eosin staining was performed on the tissue sections to evaluate the histological lesions.

Recombinant anti-tau (phospho-S396) antibody (#ab109390; Abcam, Cambridge, UK) was used for IHC. Vectastain elite Avidin-Biotin Complex kit was obtained from Vector Laboratories (Burlingame, CA, USA). Silane-coated tissue slides were deparaffinized and rehydrated with xylene and a gradually decreasing concentration of alcohol, respectively, and washed under tap water for 10 min. Washed slides were boiled in tris-ethylene diamine tetra-acetic acid buffer (pH 9.0) for 15 min in a microwave and kept at room temperature for 30 min for antigen retrieval. Antigen-retrieved tissues were then washed and incubated with 3% H_2O_2 for 10 min at room temperature. Washed slides were blocked by 5% goat serum in PBS for 1 h. Blocked tissue slides were washed with PBS and incubated with primary antibody (diluted 1:4,000) at 4°C overnight. The slides were washed in PBS and incubated with diluted secondary antibody (Vectastain) for 30 min at room temperature. The slides were washed with PBS and incubated with ABC reagent (Vectastain) for 30 min at room temperature. The slides were then washed for 5 min in PBS and

incubated in 3,3'-diaminobenzidine tetrahydrochloride solution for 10 min or until the tissues changed color. Finally, slides were washed and counterstained with hematoxylin for 1 min.

Image analysis. Slides were scanned using an Olympus VS-200 Slide Scanner (Olympus-Life Science, Tokyo, Japan). Using a custom macro in Fiji software (National Institute of Health, Bethesda, MA, USA), automated area quantification for immunolabeled sections was performed according to a previous study (26). A custom color deconvolution was performed to separate brown tau labeling from hematoxylin and eosin staining. S396 immunolabeling was evaluated using threshold analysis at intermediate intensity levels. As a measure of pathological severity, the area of immunolabeled tissue was calculated by counting the total stained pixels against the threshold. Images were tiled to apply this analysis across the entire tissue area. The results were evaluated as none when the percentage immunolabeled area of a tissue was less than 10%, light when it was 10% or more, moderate when it was 20% or more, and strong when it was 30% or more.

Results

Signs and clinical findings. The signs, clinical features, and medical records of control dogs, dogs with EAE, and dogs

Table III. Characteristics of histology and immunohistochemistry for S396-phosphorylated tau (p-tau) expression in control dogs, dogs with experimental autoimmune encephalomyelitis (EAE), and dogs with meningoencephalomyelitis of unknown etiology (MUE).

Group	Number	Brain tissue	Histological findings	Expression of p-tau*	Area quantification (%)**
Control	1	Frontal lobe	None	None	0.726
	2	Frontal lobe	None	None	1.608
EAE	1	Right frontal lobe	Lymphocytic infiltration with occasional macrophages	Strong	47.621
	2	Right parietal lobe	Lymphocytic infiltration with occasional macrophages	Strong	36.724
	3	Frontal lobe	Neutrophilic infiltration	Moderate	26.322
MUE	1	Right occipital lobe	Lymphocytic infiltration	Light	11.137
	2	Left frontal lobe	Lymphocytic infiltration with occasional histiocytes	None	3.432
	3	Left frontal lobe	Lymphocytic infiltration	None	1.728

*None, light, moderate, and strong: <10% or >10%, 20%, and 30%, respectively. **Quantification of tissue area labeled at a high intensity threshold by automated image analysis of S396 p-tau labeling.

with MUE are shown in Table I. Two control dogs (both male, Maltese and Cane Corso, 14 and 6 years old, diagnosed with myxomatous mitral valve degeneration, and heartworm infection, weighing 3 and 61.5 kg, respectively) showed no abnormalities on neurological examination. Both dogs died of chronic heart failure and heartworm infection, respectively, which were unrelated to CNS disease.

All three beagle models developed EAE. The first neurological signs of EAE were identified within an average of 28.3 days (range=12-39 days) after the first injection. The initial neurological symptom commonly identified in EAE was ataxia, which progressed rapidly to tetra-paresis. In addition, head turn, head tilt, and stuporous mental state were initially observed. Other neurological symptoms, such as respiratory paralysis and comatose mental state, were observed within 1 to 2 days after the first signs were observed. Non-specific clinical signs, including depression and anorexia, were also noted concurrently with the initial neurological signs. All three dogs with EAE underwent an acute clinical course and were euthanized at an average of 29.3 days (range=14-39 days) after the first injection due to severe CNS-related symptoms.

The MUE group consisted of two Maltese (MUE-1/MUE-2) and one Yorkshire Terrier (MUE-3). There were two females (one neutered) and one intact male, and the ages were 7, 4, and 8 years, respectively. Seizures were observed in all three dogs. Other confirmed neurological signs and non-specific clinical signs were head turn in two cases, ataxia in one case, and head tilt in one case. The onset of clinical signs was acute in all these dogs. The dogs with MUE received combination therapy with prednisone and mycophenolate mofetil. MUE-1, MUE-2, and MUE-3 had survival periods of 165, 1164, and 317 days, respectively. The cause of death in all cases with MUE was *status epilepticus* resulting from poor control of neurological symptoms despite continued treatment. MUE-1 and MUE-2 were diagnosed with NME

and MUE-3 was diagnosed with necrotizing leukoencephalitis based on the histopathological examination.

MRI and CSF analysis. The MRI and CSF findings of dogs with EAE and dogs with MUE are presented in Table II. The results of MRI and necropsy of brains are shown in Figure 1. In both the EAE and MUE groups, multifocal lesions of the white matter were confirmed as hyperintense on brain T2-weighted and FLAIR images on MRI. In T1-weighted images, there were hypo- to isointense signals in both groups. Peripheral contrast enhancement of the ill-defined lesion was only observed in the post-contrast T1-weighted image of MUE-1. Some cavitory lesions were identified in MUE-2. Gross examination of necropsy samples revealed ill-defined lesions coincident with hemorrhagic atrophy, except for MUE-1.

In CSF analysis of the EAE group, slightly or severely elevated total protein levels were observed, and neutrophilic pleocytosis was confirmed in all except for EAE-2; in EAE-2, the collection of CSF failed despite several attempts and was stopped due to bleeding. All dogs with MUE had normal total protein levels. In CSF analysis, MUE-2 and MUE-3 showed monocytic and lymphocytic pleocytosis, respectively. No abnormal finding was observed in the CSF analysis of MUE-1.

Histopathology and IHC. *Control dogs:* The expression of S396 p-tau was investigated using the same protocol by IHC assays of the forebrain of the normal dogs and compared with lesion sites from the MUE and the EAE groups. No inflammatory lesions were identified with hematoxylin and eosin staining (Figure 2A, Table III). IHC of S396 p-tau revealed no phosphorylation of tau protein in glial cells and neurons of the control group (Figure 3).

Dogs with EAE: The expression of S396 p-tau was investigated in three dogs with EAE by IHC assay. There were several pathological features similar to MUE, such as perivascular cuffs, proliferation and swelling of vascular

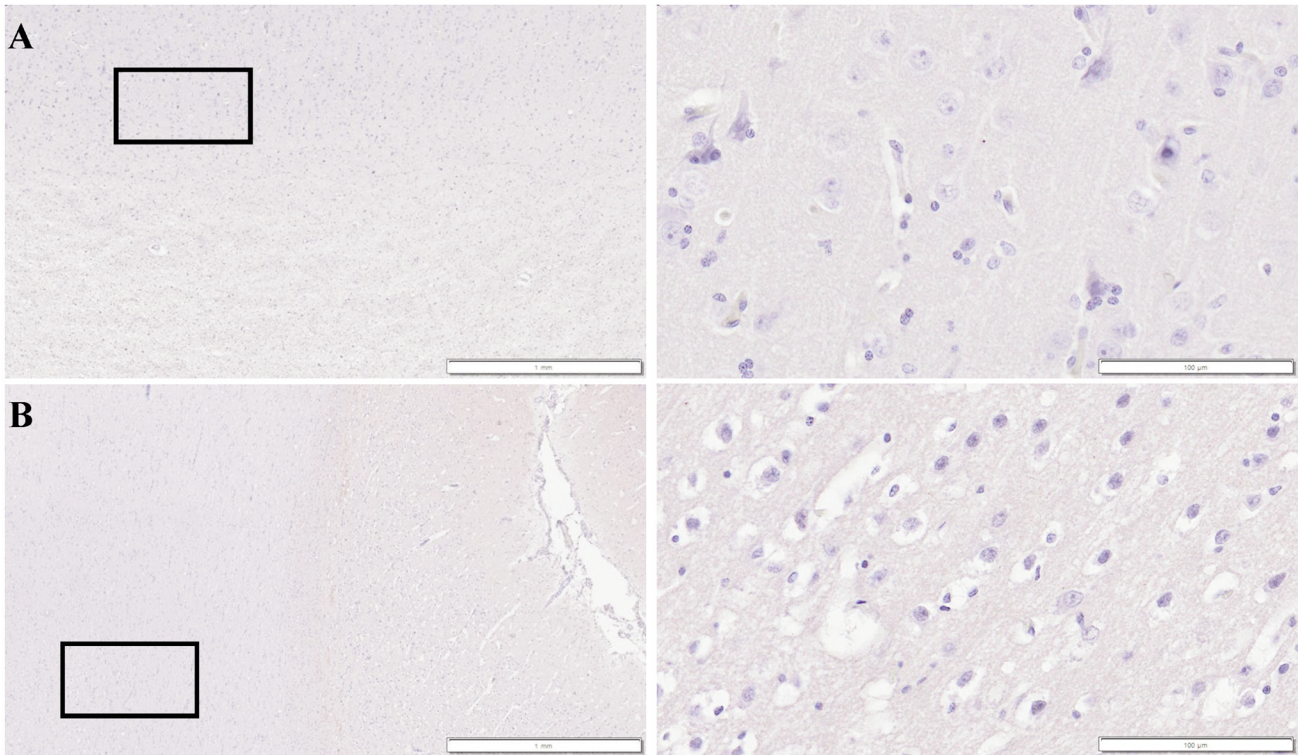


Figure 3. Immunohistochemistry of the frontal lobe of control-1 (A) and control-2 (B). S396 labeling was not observed in the frontal lobes of the control group. Boxed areas in images on the left are shown at high power on the right. The scale bar represents 1 mm (left) and 100 μ m (right).

endothelial cells, and infiltration of monocytes in the lesion sites (Figure 2B, Table III). Infiltration of neutrophils was not found in MUE lesions. S396 p-tau accumulated in glial cells and was secreted in the background in the periphery of the lesion, which extended to the white matter (Figure 4).

Dogs with MUE: The expression of S396 p-tau was investigated in three dogs with MUE by IHC assay. At lesion sites, infiltrating inflammatory cells, such as mononuclear cells, were characterized (Figure 2C and D, Table III). Inflammatory perivascular cuffing and severe neuronal necrosis were primarily identified throughout the lesions. There was swelling of vascular endothelial cells and gliosis. In MUE-1 (Figure 2C), necrosis was mild compared with the other dogs (Figure 2D). S396 p-tau accumulation in glial cells was sparsely observed in MUE-1 (Figure 5A). In the other two dogs, there was no accumulation of S396 p-tau in glial cells and neurons (Figure 5B and C).

Image analysis. The area of staining for S396 p-tau was measured as a percentage of the total slide (Table III). In the control group, the staining area was unconfirmed at 0.726% and 1.608%, respectively. The presence of p-tau was clearly confirmed in all dogs with EAE. The grade of S396 p-tau expression was confirmed as strong, strong, and moderate

for EAE-1, EAE-2, and EAE-3, respectively. Among the dogs with MUE, S396 p-tau was visually confirmed only in MUE-1, and the grade of p-tau staining was evaluated as light. Staining of p-tau in the other dogs with MUE was evaluated as none.

Discussion

This study investigated whether canine MUE and EAE models display abnormally hyperphosphorylated tau. Staining of S396 p-tau was observed in glial cells in the inflammatory lesions of all dogs with EAE and one of the three dogs with MUE. Moreover, positive staining of S396 p-tau was found in the background of lesions in dogs with EAE. These findings suggest that hyperphosphorylated tau might be involved in the pathological mechanism in canine EAE and MUE, similarly to human MS.

Previously comparable findings of clinical signs, MRI, and histopathology were noted between the canine EAE model and MUE (25), and these features were also identified in this study. In the T1-weighted images, the intracranial lesions of all dogs with EAE and dogs with MUE were confirmed to have hypo- to isointensity, and in T2-weighted and FLAIR images, they were identified as having hyperintensity. The

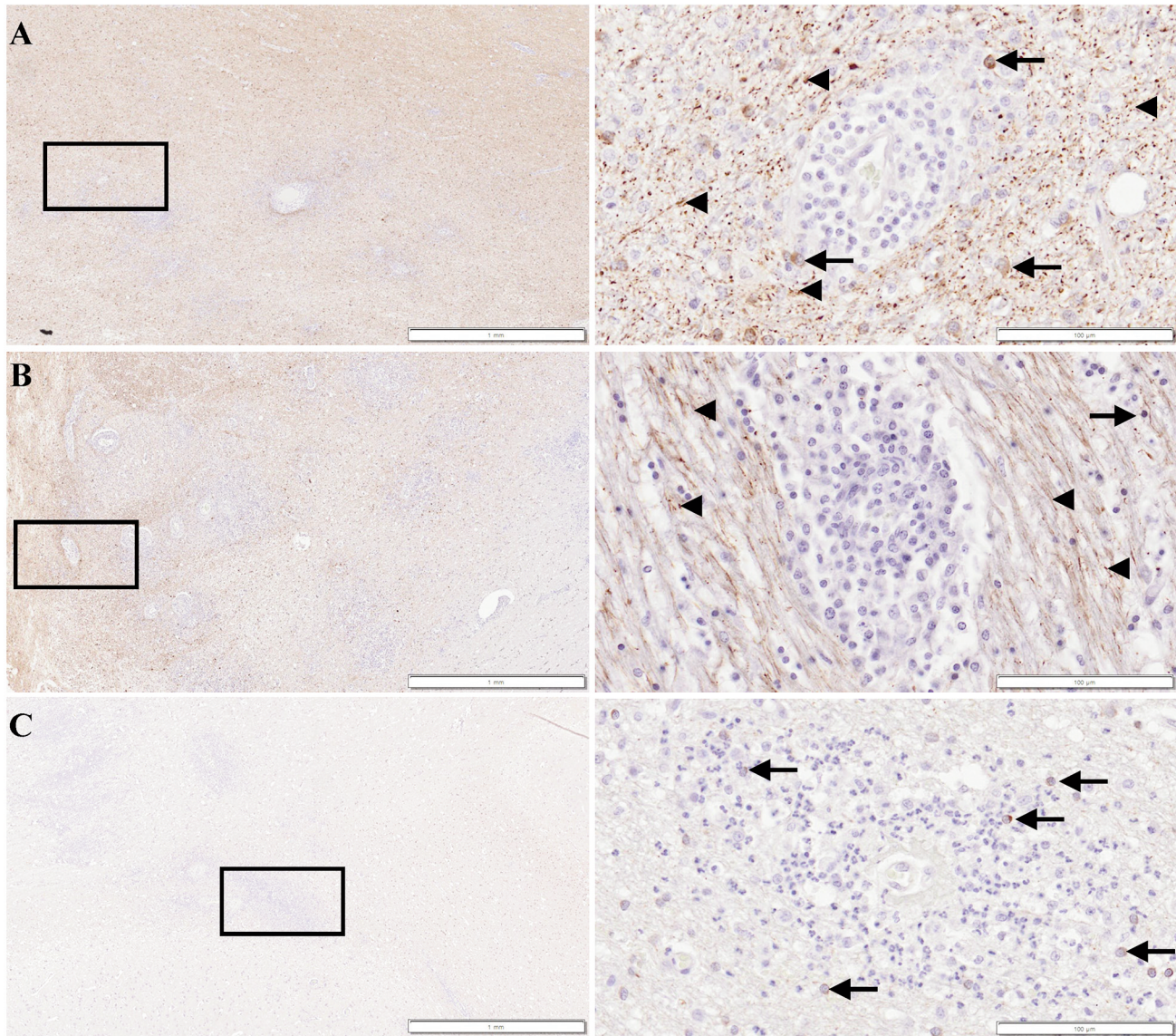


Figure 4. Immunoreactivity for S396-phosphorylated tau in the group with experimental autoimmune encephalomyelitis (EAE). **A:** In the frontal lobe of EAE-1, inflammatory perivascular cuffs and monocyte infiltration were identified. Abundant hyperphosphorylated tau accumulated in glial cells (arrows) was secreted in the background in the periphery of the lesion (arrowheads), which extended to the white matter. **B:** There was infiltration of monocytes in the lesion of the parietal lobe of EAE-2. Strong immunoreactivity was observed in glial cell cytoplasm (arrow) and the background in the periphery of the lesion (arrowheads). **C:** Moderate neutrophil and lymphocyte infiltration was observed in the frontal lobe lesion of EAE-3. There were several S396-phosphorylated tau-positive signals in the glial cells (arrows). Boxed areas in images on the left are shown at high power on the right. The scale bar represents 1 mm (left) and 100 μm (right).

lesions were mainly observed in the white matter with partial infiltration in the cortex of the brain. Identical findings were reported in MRI scans in human MS (27).

Histopathologically, perivascular inflammatory cell infiltration and parenchymal cell accumulation of inflammatory cells were mainly characterized in both canine EAE and MUE lesions (25, 28, 29). These features were also identified in this study. Furthermore, swelling of vascular endothelial cells and

astrocytic gliosis were confirmed. In previous studies, the results of IHC in the canine EAE model and MUE revealed CD3-positive macrophages and T-cells predominantly (20, 25). MS is also a typical inflammatory demyelinating disease similar to MUE in relation to T cell-mediated inflammatory pathogenesis and CD3-positive macrophages (28, 30). In MUE, astrocytes were labeled for glial fibrillary acidic protein, which is used as a marker of disease progression in human MS (29,

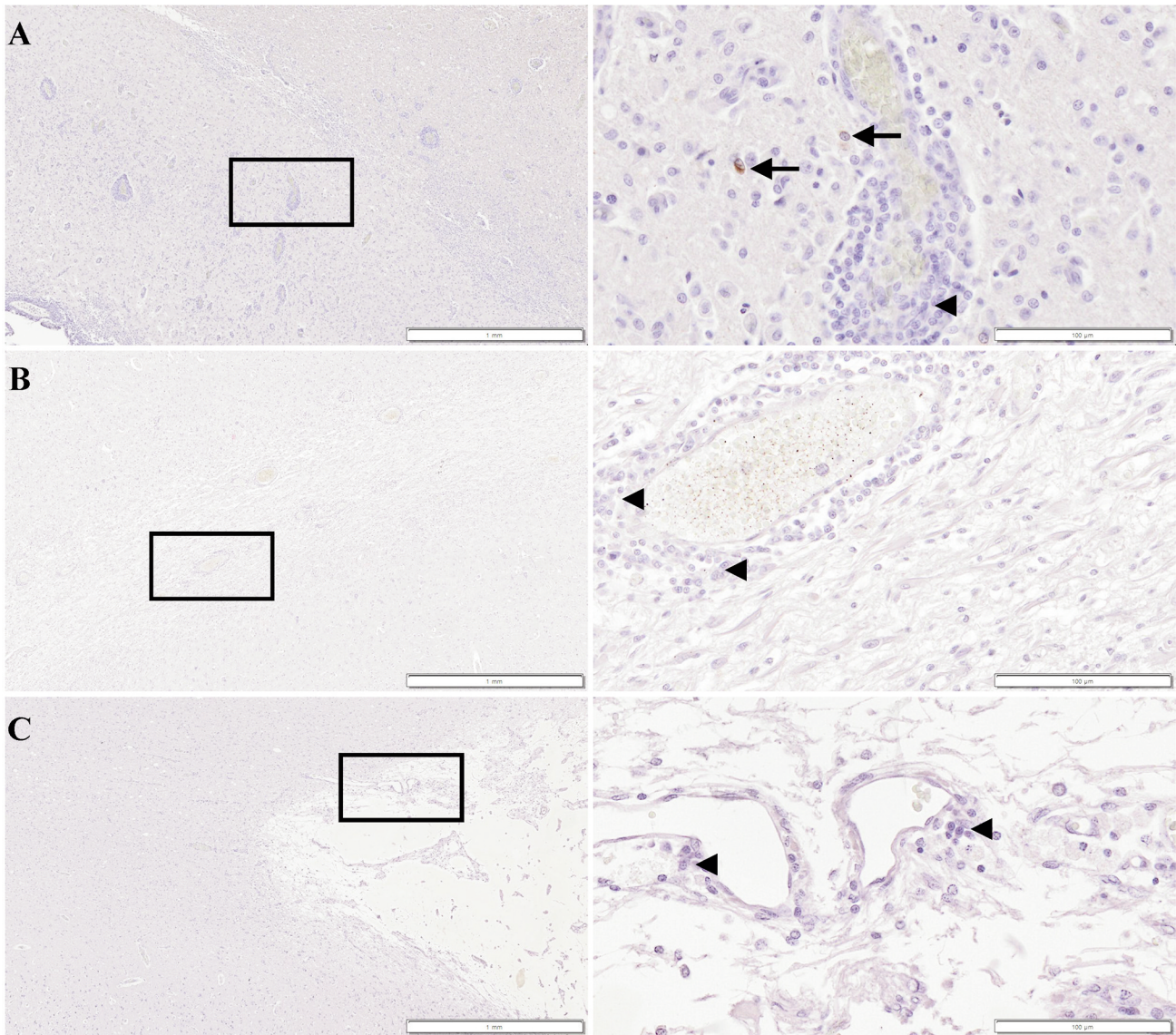


Figure 5. Expression of S396-phosphorylated tau in the group with meningoencephalomyelitis of unknown etiology (MUE). In MUE-1 (A) and MUE-2 (B), inflammatory perivascular cuffs were identified, and infiltration of lymphocytes was observed (arrowheads). In MUE-3 (C), lymphocyte infiltration was confirmed (arrowheads) and severe cell necrosis was identified. Immunoreactivity of S396 phosphorylated-tau was confirmed inside glial cells around the perivascular cuff in the occipital lobe (arrows) of MUE-1 (A). In the frontal lobe of MUE-3 (B) and MUE-2 (C), signals for S396-phosphorylated-tau were not confirmed in the lesion. Boxed areas in images on the left are shown at high power on the right. The scale bar represents 1 mm (left) and 100 μ m (right).

31, 32). Correspondingly, glial fibrillary acidic protein-positive astrocytes were present within and around the inflammatory lesions of the canine EAE model (25). Based on these findings, histopathological characteristics suggest that MUE, EAE, and MS are comparable to each other.

Hyperphosphorylated tau is expressed in glial cells such as astrocytes and oligodendrocytes in the mouse EAE model and MS (15). It triggers the loss of microtubule stability and collapse of microtubules (6). Hyperphosphorylated tau also

aggregates into pathological tau oligomers, ultimately forming pathological insoluble neurofilament tangles (6). Similarly to previous studies, the IHC distribution of S396 p-tau in the lesion of the canine EAE model was identified in this study. Therefore, canine EAE, which had the S396 p-tau-expressing lesion in this study might be speculated to have tau pathology similar to that found in previous research (15, 16, 33). In addition, S396 p-tau was expressed not only in glial cells but also in the background of the lesion. Past studies have reported

that p-tau seems to disrupt glial cells, cause inflammation stimuli, propagate to other cells, and repeat its pathology (15, 16, 33). Thus, background S396 p-tau lesions might be the cause or result of an inflammatory lesion of immune-mediated meningoencephalitis in this study. Although further studies should be conducted, pathology involving hyperphosphorylated tau appears to play a role in canine neuroinflammatory diseases similar to that in human MS.

EAE-1 and EAE-2 had similar tau immunostaining patterns, whereas EAE-3 did not. Immunostaining of tau was strong in EAE-1 and EAE-2, but moderate in EAE-3. This may be related to a variation in the brain that was used to induce EAE. Hyperphosphorylated tau protein may seed like a prion, according to a previous study (34). It is possible that hyperphosphorylated tau in the brain, which was used as the source, had an effect. EAE-2 was induced using the same brain as EAE-1, while EAE-3 was induced using the brain of EAE-1. As a result, variations in tau immunostaining patterns in this study might be attributed to differences in the brain samples used. Experiments in dogs with EAE induced utilizing the same brain should be conducted to confirm this.

The results of IHC showed positive labeling of p-tau in all dogs with EAE and one dog with MUE (MUE-1). Contrary to dogs with EAE, S396 p-tau was not identified in the other two dogs with MUE. The absence of staining for S396 p-tau in dogs with MUE may be due to several factors. As mentioned above, although MS, EAE, and MUE share various histopathological characteristics, there are also subtle differences (22). The pathological hallmark of MS and EAE is a lesion consisting of perivascular infiltration of inflammatory cells, with subsequent demyelination (28, 35, 36). Demyelination also occurs in MUE, but necrosis is a key pathology of MUE (22, 29). Thus, tau involvement in the pathological course might also be different between MUE and EAE because MUE may have a pathology partially different from that of MS.

Phosphorylation of tau protein may occur at several amino acid residues (6). In humans, the anti-phospho-tau (pS202/pT205) monoclonal antibody (AT8) has been mainly used in tau pathology studies, as it has been shown to be involved in the oligomerization of tau in Alzheimer's and MS in humans (16, 37). Although studies on tau pathology in veterinary medicine have been limited, one study reported that the S396 epitope is more involved in the pathology of canine cognitive dysfunction syndrome than the AT8 epitope, which is associated with neurofibrillary tangles (26). Compared with AT8, the S396 epitope is hyperphosphorylated at an early stage of disease (38-40). The only dog with MUE with a positive result for S396 p-tau was necropsied at 165 days after confirmation of onset, while the other dogs with MUE were necropsied at 304 and 1,165 days, respectively, after the first signs were identified. Due to the prolongation of MUE, it is likely that a late epitope rather than an early epitope was

mainly involved, or that other tau protein epitopes were involved in MUE pathology. Therefore, further studies are needed on other p-tau epitopes, such as AT8 and AT180.

In this study, all dogs with MUE were treated with immunosuppressants, such as prednisolone and mycophenolate mofetil, from diagnosis to death. Previous studies reported that hyperphosphorylation of tau was induced by hyperactivation of the mammalian target of rapamycin (mTOR) pathway (41, 42). Furthermore, it is well known that glucocorticoids, such as prednisolone, inhibit the mTOR pathway (43, 44). In addition, a study reported reduced p-tau immunostaining in a mouse EAE model which was treated with prednisolone (14). Altogether, we suspected that p-tau was not expressed in dogs with MUE due to long-term immunosuppressive treatment. Additionally, it was presumed that a small amount of p-tau was confirmed for MUE-1 because the treatment period was relatively short compared with that of the other dogs with MUE.

According to a previous NME study (20), NME lesions can be divided into three stages depending on the extent of tissue necrosis and the severity of the inflammatory response. Compared with MUE-1, moderate tissue necrosis and severe inflammatory changes were noted in the histopathological examination of MUE-3. In MUE-2, severe malacic changes and cavitations were dominant, although inflammatory changes were less compared with MUE-1 and MUE-3. Based on the histopathological features and the survival time, MUE-2 and MUE-3 were considered to be in the late stages of NME compared with MUE-1. EAE models were euthanized within 2 days of symptom confirmation; hence, the disease was in its infancy, and necrosis had hardly progressed. Accumulation of S396 p-tau was mainly found inside glial cells in MS, but it was not possible to confirm this in MUE because most of the glial cells were in a necrotic state. To confirm whether such accumulation also occurs in MUE, further studies on brains in the early stage of MUE are needed.

This study had several limitations. Firstly, the sample group was too small to generalize the relationship between MUE and tau protein. The number of healthy controls, in particular, was insufficient, as was the number of samples by the type of MUE. Additional studies should be carried out with a larger number of samples. Secondly, only one type of p-tau antibody was utilized. As mentioned above, hyperphosphorylation can occur at several amino acid residues. In this study, only the anti-tau (phospho-S396) antibody was used for IHC. The possibility of expression of different p-tau isoforms cannot be excluded. Therefore, studies including other p-tau antibodies such as AT8 and AT180 should be conducted. Finally, there were no validations in untreated dogs with MUE and testing in dogs with MUE at an initial stage. Significant discrepancies in the outcomes might be caused by differences in immunosuppressive treatment and the extent of brain tissue necrosis. Brain samples from initial MUE were not available. Therefore, further research is required with samples that fulfill these criteria.

Conclusion

This study demonstrates abnormal expression of p-tau in dogs with EAE and dogs with MUE compared with normal dogs. Moreover, the p-tau distribution in both groups was similar to that of human MS. Together, these results implicate tau dysfunction in canine EAE and MUE, as in human MS. To the best of the authors' knowledge, this is the first study suggesting that tau pathology might be involved in neuroinflammation in dogs. This study provides a platform for further investigations on the contribution of hyperphosphorylated tau in canine MUE. Furthermore, the canine EAE model could be used as a model for tau pathology for human MS.

Conflicts of Interest

The Authors declare that the research was conducted in the absence of any commercial or financial relationships that could be construed as a potential conflict of interest.

Authors' Contributions

MS and YC contributed to the conception and design of the research. SK and SK performed the experiments and interpreted the results. TY, YK, and DL were involved in data collection. BTK, HK, MPY, and SK contributed to the editing, revising, and final approval of the article. All Authors critically revised the article and read and approved the final version.

Acknowledgements

This work was supported by a National Research Foundation of Korea (NRF) grant funded by the Korean government (MSIT) (No. 2021R1A2C1012058) and the Basic Research Lab Program (2022R1A4A1025557) through the NRF of Korea funded by the Ministry of Science and ICT.

References

- Ballatore C, Lee VM and Trojanowski JQ: Tau-mediated neurodegeneration in Alzheimer's disease and related disorders. *Nat Rev Neurosci* 8(9): 663-672, 2007. PMID: 17684513. DOI: 10.1038/nrn2194
- Avila J, Lucas JJ, Perez M and Hernandez F: Role of tau protein in both physiological and pathological conditions. *Physiol Rev* 84(2): 361-384, 2004. PMID: 15044677. DOI: 10.1152/physrev.00024.2003
- Huang Y, Wu Z and Zhou B: Behind the curtain of tauopathy: a show of multiple players orchestrating tau toxicity. *Cell Mol Life Sci* 73(1): 1-21, 2016. PMID: 26403791. DOI: 10.1007/s00018-015-2042-8
- Kolarova M, García-Sierra F, Bartos A, Ricny J and Ripova D: Structure and pathology of tau protein in Alzheimer disease. *Int J Alzheimers Dis* 2012: 731526, 2012. PMID: 22690349. DOI: 10.1155/2012/731526
- Goedert M and Spillantini M: Synucleinopathies and Tauopathies. *Basic Neurochemistry*: 829-843, 2022. DOI: 10.1016/B978-0-12-374947-5.00047-X
- Wang JZ, Xia YY, Grundke-Iqbal I and Iqbal K: Abnormal hyperphosphorylation of tau: sites, regulation, and molecular mechanism of neurofibrillary degeneration. *J Alzheimers Dis* 33 Suppl 1: S123-S139, 2013. PMID: 22710920. DOI: 10.3233/JAD-2012-129031
- Wu XL, Piña-Crespo J, Zhang YW, Chen XC and Xu HX: Tau-mediated neurodegeneration and potential implications in diagnosis and treatment of Alzheimer's disease. *Chin Med J (Engl)* 130(24): 2978-2990, 2017. PMID: 29237931. DOI: 10.4103/0366-6999.220313
- Iqbal K, Gong CX and Liu F: Hyperphosphorylation-induced tau oligomers. *Front Neurol* 4: 112, 2013. PMID: 23966973. DOI: 10.3389/fneur.2013.00112
- Shafiei SS, Guerrero-Muñoz MJ and Castillo-Carranza DL: Tau oligomers: Cytotoxicity, propagation, and mitochondrial damage. *Front Aging Neurosci* 9: 83, 2017. PMID: 28420982. DOI: 10.3389/fnagi.2017.00083
- Johnson GV and Stoothoff WH: Tau phosphorylation in neuronal cell function and dysfunction. *J Cell Sci* 117(Pt 24): 5721-5729, 2004. PMID: 15537830. DOI: 10.1242/jcs.01558
- Bandyopadhyay B, Li G, Yin H and Kuret J: Tau aggregation and toxicity in a cell culture model of tauopathy. *J Biol Chem* 282(22): 16454-16464, 2007. PMID: 17428800. DOI: 10.1074/jbc.M700192200
- Lee DC, Rizer J, Selenica ML, Reid P, Kraft C, Johnson A, Blair L, Gordon MN, Dickey CA and Morgan D: LPS- induced inflammation exacerbates phospho-tau pathology in rTg4510 mice. *J Neuroinflammation* 7: 56, 2010. PMID: 20846376. DOI: 10.1186/1742-2094-7-56
- Zilka N, Kazmerova Z, Jadhav S, Neradil P, Madari A, Obetkova D, Bugos O and Novak M: Who fans the flames of Alzheimer's disease brains? Misfolded tau on the crossroad of neurodegenerative and inflammatory pathways. *J Neuroinflammation* 9: 47, 2012. PMID: 22397366. DOI: 10.1186/1742-2094-9-47
- Schneider A, Araújo GW, Trajkovic K, Herrmann MM, Merkler D, Mandelkow EM, Weissert R and Simons M: Hyperphosphorylation and aggregation of tau in experimental autoimmune encephalomyelitis. *J Biol Chem* 279(53): 55833-55839, 2004. PMID: 15494405. DOI: 10.1074/jbc.M409954200
- Anderson JM, Hampton DW, Patani R, Pryce G, Crowther RA, Reynolds R, Franklin RJ, Giovannoni G, Compston DA, Baker D, Spillantini MG and Chandran S: Abnormally phosphorylated tau is associated with neuronal and axonal loss in experimental autoimmune encephalomyelitis and multiple sclerosis. *Brain* 131(Pt 7): 1736-1748, 2008. PMID: 18567922. DOI: 10.1093/brain/awn119
- Anderson JM, Patani R, Reynolds R, Nicholas R, Compston A, Spillantini MG and Chandran S: Abnormal tau phosphorylation in primary progressive multiple sclerosis. *Acta Neuropathol* 119(5): 591-600, 2010. PMID: 20306268. DOI: 10.1007/s00401-010-0671-4
- Islas-Hernandez A, Aguilar-Talamantes HS, Bertado-Cortes B, Mejia-delCastillo GJ, Carrera-Pineda R, Cuevas-Garcia CF and Garcia-delaTorre P: BDNF and Tau as biomarkers of severity in multiple sclerosis. *Biomark Med* 12(7): 717-726, 2018. PMID: 29865854. DOI: 10.2217/bmm-2017-0374
- Tipold A: Diagnosis of inflammatory and infectious diseases of the central nervous system in dogs: a retrospective study. *J Vet Intern Med* 9(5): 304-314, 1995. PMID: 8531175. DOI: 10.1111/j.1939-1676.1995.tb01089.x

- 19 Granger N, Smith PM and Jeffery ND: Clinical findings and treatment of non-infectious meningoencephalomyelitis in dogs: a systematic review of 457 published cases from 1962 to 2008. *Vet J* 184(3): 290-297, 2010. PMID: 19410487. DOI: 10.1016/j.tvjl.2009.03.031
- 20 Suzuki M, Uchida K, Morozumi M, Hasegawa T, Yanai T, Nakayama H and Tateyama S: A comparative pathological study on canine necrotizing meningoencephalitis and granulomatous meningoencephalomyelitis. *J Vet Med Sci* 65(11): 1233-1239, 2003. PMID: 14665754. DOI: 10.1292/jvms.65.1233
- 21 Sospedra M and Martin R: Immunology of multiple sclerosis. *Annu Rev Immunol* 23: 683-747, 2005. PMID: 15771584. DOI: 10.1146/annurev.immunol.23.021704.115707
- 22 Greer KA, Wong AK, Liu H, Famula TR, Pedersen NC, Ruhe A, Wallace M and Neff MW: Necrotizing meningoencephalitis of Pug dogs associates with dog leukocyte antigen class II and resembles acute variant forms of multiple sclerosis. *Tissue Antigens* 76(2): 110-118, 2010. PMID: 20403140. DOI: 10.1111/j.1399-0039.2010.01484.x
- 23 Thomas L, Paterson PY and Smithwick B: Acute disseminated encephalomyelitis following immunization with homologous brain extracts; studies on the role of a circulating antibody in the production of the condition in dogs. *J Exp Med* 92(2): 133-152, 1950. PMID: 15428583. DOI: 10.1084/jem.92.2.133
- 24 Kuharik MA, Edwards MK, Farlow MR, Becker GJ, Azzarelli B, Klatte EC, Augustyn GT and Dreesen RG: Gd-enhanced MR imaging of acute and chronic experimental demyelinating lesions. *AJNR Am J Neuroradiol* 9(4): 643-648, 1988. PMID: 3135711.
- 25 Moon JH, Jung HW, Lee HC, Jeon JH, Kim NH, Sur JH, Ha J and Jung DI: A study of experimental autoimmune encephalomyelitis in dogs as a disease model for canine necrotizing encephalitis. *J Vet Sci* 16(2): 203-211, 2015. PMID: 25269720. DOI: 10.4142/jvs.2015.16.2.203
- 26 Abey A, Davies D, Goldsbury C, Buckland M, Valenzuela M and Duncan T: Distribution of tau hyperphosphorylation in canine dementia resembles early Alzheimer's disease and other tauopathies. *Brain Pathol* 31(1): 144-162, 2021. PMID: 32810333. DOI: 10.1111/bpa.12893
- 27 Thompson AJ, Banwell BL, Barkhof F, Carroll WM, Coetzee T, Comi G, Correale J, Fazekas F, Filippi M, Freedman MS, Fujihara K, Galletta SL, Hartung HP, Kappos L, Lublin FD, Marrie RA, Miller AE, Miller DH, Montalban X, Mowry EM, Sorensen PS, Tintoré M, Traboulsee AL, Trojano M, Uitdehaag BMJ, Vukusic S, Waubant E, Weinshenker BG, Reingold SC and Cohen JA: Diagnosis of multiple sclerosis: 2017 revisions of the McDonald criteria. *Lancet Neurol* 17(2): 162-173, 2018. PMID: 29275977. DOI: 10.1016/S1474-4422(17)30470-2
- 28 Lassmann H: Multiple sclerosis pathology. *Cold Spring Harb Perspect Med* 8(3): a028936, 2018. PMID: 29358320. DOI: 10.1101/cshperspect.a028936
- 29 Park ES, Uchida K and Nakayama H: Comprehensive immunohistochemical studies on canine necrotizing meningoencephalitis (NME), necrotizing leukoencephalitis (NLE), and granulomatous meningoencephalomyelitis (GME). *Vet Pathol* 49(4): 682-692, 2012. PMID: 22262353. DOI: 10.1177/0300985811429311
- 30 Garg N and Smith TW: An update on immunopathogenesis, diagnosis, and treatment of multiple sclerosis. *Brain Behav* 5(9): e00362, 2015. PMID: 26445701. DOI: 10.1002/brb3.362
- 31 Axelsson M, Malmeström C, Nilsson S, Haghighi S, Rosengren L and Lycke J: Glial fibrillary acidic protein: a potential biomarker for progression in multiple sclerosis. *J Neurol* 258(5): 882-888, 2011. PMID: 21197541. DOI: 10.1007/s00415-010-5863-2
- 32 Högel H, Rissanen E, Barro C, Matilainen M, Nylund M, Kuhle J and Airas L: Serum glial fibrillary acidic protein correlates with multiple sclerosis disease severity. *Mult Scler* 26(2): 210-219, 2020. PMID: 30570436. DOI: 10.1177/1352458518819380
- 33 Shriver LP and Dittel BN: T-cell-mediated disruption of the neuronal microtubule network: correlation with early reversible axonal dysfunction in acute experimental autoimmune encephalomyelitis. *Am J Pathol* 169(3): 999-1011, 2006. PMID: 16936273. DOI: 10.2353/ajpath.2006.050791
- 34 Gerson JE and Kaye R: Formation and propagation of tau oligomeric seeds. *Front Neurol* 4: 93, 2013. PMID: 23882255. DOI: 10.3389/fneur.2013.00093
- 35 Popescu BF, Pirko I and Lucchinetti CF: Pathology of multiple sclerosis: where do we stand? *Continuum (Minneapolis)* 19(4 Multiple Sclerosis): 901-921, 2013. PMID: 23917093. DOI: 10.1212/01.CON.0000433291.23091.65
- 36 Constantinescu CS, Farooqi N, O'Brien K and Gran B: Experimental autoimmune encephalomyelitis (EAE) as a model for multiple sclerosis (MS). *Br J Pharmacol* 164(4): 1079-1106, 2011. PMID: 21371012. DOI: 10.1111/j.1476-5381.2011.01302.x
- 37 Usenovic M, Niroomand S, Drolet RE, Yao L, Gaspar RC, Hatcher NG, Schachter J, Renger JJ and Parmentier-Batteur S: Internalized tau oligomers cause neurodegeneration by inducing accumulation of pathogenic tau in human neurons derived from induced pluripotent stem cells. *J Neurosci* 35(42): 14234-14250, 2015. PMID: 26490863. DOI: 10.1523/JNEUROSCI.1523-15.2015
- 38 Augustinack JC, Schneider A, Mandelkow EM and Hyman BT: Specific tau phosphorylation sites correlate with severity of neuronal cytopathology in Alzheimer's disease. *Acta Neuropathol* 103(1): 26-35, 2002. PMID: 11837744. DOI: 10.1007/s004010100423
- 39 Gong CX and Iqbal K: Hyperphosphorylation of microtubule-associated protein tau: a promising therapeutic target for Alzheimer disease. *Curr Med Chem* 15(23): 2321-2328, 2008. PMID: 18855662. DOI: 10.2174/092986708785909111
- 40 Mondragón-Rodríguez S, Perry G, Luna-Muñoz J, Acevedo-Aquino MC and Williams S: Phosphorylation of tau protein at sites Ser(396-404) is one of the earliest events in Alzheimer's disease and Down syndrome. *Neuropathol Appl Neurobiol* 40(2): 121-135, 2014. PMID: 24033439. DOI: 10.1111/nan.12084
- 41 Caccamo A, Majumder S, Richardson A, Strong R and Oddo S: Molecular interplay between mammalian target of rapamycin (mTOR), amyloid-beta, and Tau: effects on cognitive impairments. *J Biol Chem* 285(17): 13107-13120, 2010. PMID: 20178983. DOI: 10.1074/jbc.M110.100420
- 42 Mueed Z, Tandon P, Maurya SK, Deval R, Kamal MA and Poddar NK: Tau and mTOR: The hotspots for multifarious diseases in Alzheimer's development. *Front Neurosci* 12: 1017, 2019. PMID: 30686983. DOI: 10.3389/fnins.2018.01017
- 43 Baida G, Bhalla P, Kirsanov K, Lesovaya E, Yakubovskaya M, Yuen K, Guo S, Lavker RM, Readhead B, Dudley JT and Budunova I: REDD1 functions at the crossroads between the therapeutic and adverse effects of topical glucocorticoids. *EMBO Mol Med* 7(1): 42-58, 2015. PMID: 25504525. DOI: 10.15252/emmm.201404601

Received January 29, 2023
 Revised February 20, 2023
 Accepted February 23, 2023